Vascular Adhesion Protein-1 Blockade Suppresses Ocular Inflammation After Retinal Laser Photocoagulation in Mice

Takashi Matsuda,[1] Kousuke Noda,[1,2] Miyuki Murata,[1,2] Akiko Kawasaki,[3] Atsuhiro Kanda,[1,2] Yukihiko Mashima,[4] and Susumu Ishida[1,2]

[1]Laboratory of Ocular Cell Biology & Visual Science, Faculty of Medicine and Graduate School of Medicine, Hokkaido University, Sapporo, Japan
[2]Department of Ophthalmology, Faculty of Medicine and Graduate School of Medicine, Hokkaido University, Sapporo, Japan
[3]Sucampo Pharma, LLC, Tokyo, Japan
[4]Department of Ophthalmology, Keio University School of Medicine, Tokyo, Japan

Correspondence: Kousuke Noda, Department of Ophthalmology, Faculty of Medicine and Graduate School of Medicine, Hokkaido University, N-15, W-7, Kita-ku, Sapporo 060-8638, Japan; nodako@med.hokudai.ac.jp.

Submitted: January 26, 2017
Accepted: May 29, 2017

Citation: Matsuda T, Noda K, Murata M, et al. Vascular adhesion protein-1 blockade suppresses ocular inflammation after retinal laser photocoagulation in mice. *Invest Ophthalmol Vis Sci*. 2017;58:3254–3261. DOI: 10.1167/iovs.17-21555

Purpose. To investigate the effect of the vascular adhesion protein-1 (VAP-1) inhibitor RTU-1096 on retinal morphologic changes and ocular inflammation after retinal laser photocoagulation in mice.

Methods. C57BL/6JJcl mice were fed a diet containing RTU-1096, a specific inhibitor for VAP-1, or a control diet ad libitum for 7 days. Laser photocoagulation was performed on the peripheral retina of the animals. The semicarbazide sensitive amine oxidase (SSAO) activities in plasma and chorioretinal tissues were measured. Optical coherence tomography (OCT) images were acquired before and at 1, 3, and 7 days after laser photocoagulation, and thickness of the individual retinal layers was measured. Intravitreal leukocyte infiltration was assessed by histologic analysis. The expression level of intercellular adhesion molecule-1 (*ICAM-1*) in retinal tissues were examined by quantitative real-time PCR.

Results. One day after laser photocoagulation, the thickness of the outer nuclear layer (ONL) increased in the laser group compared with in the control group, and RTU-1096 administration abrogated the ONL thickening. Histologic analysis and OCT observation revealed that laser photocoagulation caused infiltration of inflammatory cells and the appearance of hyperreflective foci at the vitreoretinal surface, both of which were suppressed by RTU-1096 administration. In addition, systemic administration of RTU-1096 reduced upregulation of the leukocyte adhesion molecules ICAM-1 in the retina.

Conclusions. The current data indicate that VAP-1/SSAO inhibition may be a potential therapeutic strategy for the prevention of macular edema secondary to scatter laser photocoagulation in patients with ischemic retinal diseases such as diabetic retinopathy.

Keywords: vascular adhesion protein-1, laser photocoagulation, macular edema, diabetic retinopathy

Diabetic retinopathy (DR) is a leading cause of blindness worldwide.[1,2] Retinal microvascular complications induced by diabetes result in obliteration of retinal capillaries, retinal ischemia, and eventual ocular neovascularization. Vascular endothelial growth factor, a potent angiogenic factor generated in ischemic retina, is responsible for vascular permeability leading to diabetic macular edema (DME)[3,4] and ocular neovascularization leading to proliferative diabetic retinopathy (PDR).[5,6] As a corollary, anti-VEGF agents have emerged as a part of first-line treatment for DME[7,8] and an adjunct therapy to vitrectomy and laser photocoagulation for PDR.[9]

Prior to the discovery of VEGF, laser photocoagulation had been applied to the treatment of DR nearly for half a century, and multicenter trials demonstrated that scatter laser photocoagulation effectively reduced the vision loss risk in patients with advanced PDR,[10–12] presumably due to the reduced VEGF production in ischemic retina. However, scatter laser photocoagulation also causes destruction of retinal tissues.[13] In addition, thermal burn caused by laser photocoagulation worsens pre-existing ME and induces post-photocoagulation ME in some DR cases,[14,15] particularly when applied rapidly.[15] Intravitreal triamcinolone or anti-VEGF agent injections were reported to reduce the risk of deterioration of ME after scatter laser photocoagulation.[16] However, intravitreal injection carries the potential risk of endophthalmitis,[17] an intraocular infection with vision threatening consequences, and therefore a therapeutic strategy to prevent postlaser ME via oral or systemic administration is of great significance.

Vascular adhesion protein-1 (VAP-1) is a sialylated glycoprotein expressed on the vascular endothelial cells of human tissues and is involved in the transmigration step of leukocyte trafficking.[18,19] We previously reported that VAP-1 is expressed on retinal vessel endothelium and it plays a critical role in the eye during acute inflammatory conditions[20] and in the early stage of DR.[21] In addition to its role as an adhesion molecule, VAP-1 also possesses semicarbazide sensitive amine oxidase (SSAO) activity, which converts primary amines to the

corresponding aldehydes with the release of ammonia and hydrogen peroxide,[22] one of the reactive oxygen species that induces oxidative stress. Thus, VAP-1/SSAO is a 'moonlighting protein' as a single molecule with multiple functions for both chronic inflammation and oxidative stress. Because both inflammation[23,24] and oxidative stress[25] are involved in the development of DME and postlaser ME, VAP-1/SSAO is considered a potential drug target for visual loss prevention after scatter laser photocoagulation.

The aim of this study was to investigate the effect of the VAP-1/SSAO inhibitor RTU-1096 on ocular inflammation and retinal morphologic changes after laser photocoagulation in mice.

Methods

Animals

In this study, C57BL/6JJcl mice (8-week-old males; CLEA Japan, Tokyo, Japan) were used in accordance with the ARVO Statement for the Use of Animals in Ophthalmic and Vision Research, and the Ethics Review Committee for Animal Experimentation of Hokkaido University approved this study (#15-0083). The animals were fed a standard mouse chow CRF-1 (Oriental Yeast Co. Ltd., Tokyo, Japan) containing the VAP-1 specific inhibitor RTU-1096 (0.2475 %; Sucampo Pharma, LLC, Tokyo, Japan) or CRF-1 without RTU-1096, ad libitum for 7 days before laser photocoagulation. Whereas IC50 of chemical inhibitor RTU-1096 against VAP-1/SSAO is 0.9 nM, its IC50 against monoamine oxidase (MAO)-A and MAO-B were more than 100 μM, indicating the specific inhibitory property of RTU-1096 on VAP-1/SSAO. The administration of RTU-1096 or control chow was continued until the end of the study.

Laser Photocoagulation

The animals were anesthetized with an intraperitoneal injection of xylazine hydrochloride (0.2 mg/mL) and ketamine hydrochloride (1 mg/mL) and the pupils were then dilated with 0.5 % tropicamide and 2.5 % phenylephrine hydrochloride. Laser photocoagulation (100 shots, spot size, 100 μm; duration, 0.03 seconds; power, 50 mW) was delivered to the peripheral retina (4 disc diameters away from optic disc, Fig. 1) through a slit-lamp biomicroscope (Novus Spectra, Yokneam, Israel).

SSAO Activity Assay

Seven days after laser photocoagulation, mice were deeply anesthetized and blood was collected into EDTA by cardiac puncture. The blood samples were centrifuged at 1800 *g* for 15 minutes at 4°C, and plasma was collected and stored at −80°C. Subsequently, the eyeballs were enucleated and chorioretinal tissue samples were harvested. Protein concentration was determined using the Quick Start Protein Assay Kit (Bio-Rad Laboratories, Hercules, CA, USA). The SSAO activities in plasma and chorioretinal tissues were determined as described previously.[20]

In Vivo Morphologic Analysis

After the anesthesia and pupil dilation, optical coherence tomography (OCT) images were acquired before and at 1, 3, and 7 days after laser photocoagulation using the Spectralis OCT system (Heidelberg Engineering, Heidelberg, Germany). To prevent corneal desiccation during OCT image acquisition, saline solution was applied bilaterally every 5 minutes. Using the eye tracking and retest function of Spectralis, horizontal

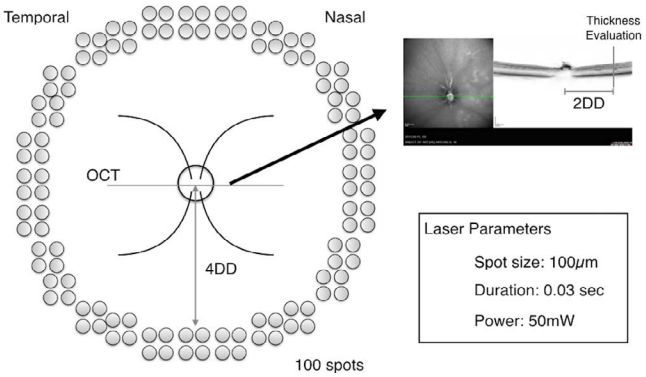

Figure 1. Schematic illustration of laser photocoagulation and OCT image acquisition. Laser photocoagulation was delivered to the peripheral retina (4 disc diameters away from optic disc, 100 shots per eye) through a slit-lamp biomicroscope. The conditions were: spot size, 100 μm; duration, 0.03 seconds; power, 50 mW. Using the eye tracking and retest function of Spectralis, horizontal OCT images passing through the optic nerve head were taken at the identical portion during the study, and total retinal thickness and individual retinal layer thickness were quantified at the nasal side of the retina (2 disc diameters away from optic disc).

OCT images passing through the optic nerve head were taken at identical locations during the study (Fig. 1). Total retinal thickness and individual retinal layer thickness, including the combination of retinal nerve fiber, ganglion cell, and inner plexiform layers (RNFL/GC/IPL), inner nuclear layer (INL), outer plexiform layer (OPL), outer nuclear layer (ONL), and the complex from the outer limiting membrane to retinal pigment epithelium posterior border (OLM/RPE), were manually quantified at the nasal side of the retina (2 disc diameters away from optic disc, Fig. 1).

Furthermore, the number of hyperreflective foci emerging at the vitreoretinal surface was evaluated. One day after laser photocoagulation, a single OCT image passing through the optic nerve head was taken and two examiners (KN and TM) counted the hyperreflective foci at the vitreoretinal surface in a masked fashion.

Histologic Analysis of Leukocyte Infiltration

The number of leukocytes infiltrating into the vitreous was assessed. Briefly, 1 day after laser photocoagulation, the animals were euthanized by an anesthesia overdose and the eyeballs were enucleated. Mouse eyeballs were fixed in 4% paraformaldehyde for 30 minutes on ice, incubated in an increasing concentration of PBS/sucrose, and embedded in frozen section compound (Leica, Exton, PA, USA). Frozen sections of 10-μm thickness were prepared at a distance of 100 μm from each other with the middle section passing through the optic nerve. Three 10-μm sections were stained with hematoxylin and eosin (H&E), and the number of infiltrating cells in the vitreous cavity was counted, as previously described.[20]

Quantitative Real-Time Polymerase Chain Reaction

The expression levels of leukocyte adhesion molecules in retinal tissues obtained from the animals were examined by quantitative real-time PCR. In brief, the retinal tissues were obtained from the control and laser groups with or without administration of RTU-1096 (0.2475%) at 1 day after laser photocoagulation and stored in RNA Later solution (Thermo Fisher Scientific, Waltham, MA, USA) for RNA stabilization. The retinal tissues were homogenized in TRI Reagent (Molecular

Investigative Ophthalmology & Visual Science

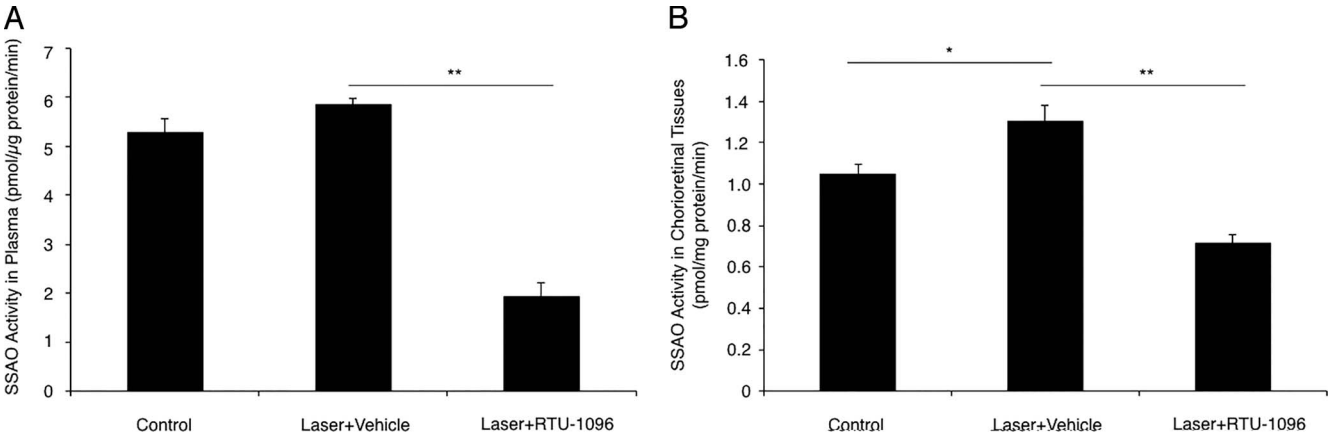

FIGURE 2. Enzymatic activity of VAP-1/SSAO in plasma and chorioretinal tissues. (**A**) Semicarbazide sensitive amine oxidase activity in plasma samples of control and laser-treated animals with or without VAP-1 inhibition, 7 days after laser photocoagulation ($n = 10$). (**B**) Semicarbazide sensitive amine oxidase activity in chorioretinal tissue samples of control and laser-treated animals with or without VAP-1 inhibition, 7 days after laser photocoagulation ($n = 18$–19). The enzymatic activity of VAP-1/SSAO was measured by radiochemistry. Values are mean ± SEM. $^{*}P < 0.05$, $^{**}P < 0.01$.

Research Center, Inc., Cincinnati, OH, USA) and total RNA was prepared according to the manufacturer's protocol. Equal amounts of total RNA extracted from samples were reverse-transcribed with GoScript Reverse Transcriptase (Promega, Madison, WI, USA) at 42°C for 1 hour in a 20-μL reaction volume. Subsequently, a real-time PCR assay for intercellular adhesion molecule-1 (*ICAM-1*) expression was performed (SYBR Green method, with the GoTaq qPCR Master Mix; Promega), according to the manufacturer's protocol. The primer sequences used for real-time PCR and the expected size of the amplification products are as follows: 5′-CCTGTTTC CTGGCTCTGAAG-3′ (forward) and 5′-GTCTGCTGAG ACCCCTCTTG-3′ (reverse) for *ICAM-1*, and 5′-AGGTCGGTGT GAACGGATTTG-3′ (forward) and 5′-TGTAGACCATGTAGTTG AGGTCA-3′ (reverse) for Glyceraldehyde-3-phosphate dehydrogenase (*GAPDH*). The cycling conditions used were 95°C, 2 minutes; followed by 95 °C, 15 seconds and 60 °C, 60 seconds for 40 cycles. All data were calculated by the ΔΔCt method with *GAPDH* as the normalization control.

Magnetic Luminex Assay

The protein level of ICAM-1 in the mouse retina was measured using mouse magnetic Luminex assay (R&D systems, Minneapolis, MN, USA), according to the manufacturer's protocol. Briefly, microparticle coated with mouse ICAM-1 antibody, tissue lysate of retina, and standards were added to a 96-well plate. Following incubation, plates were washed and a biotin antibody cocktail was added. After incubation for 1 hour, plates were washed and streptavidin-phycoerythrin was added for 30 minutes, followed by a final wash and resuspension in wash buffer, and analyzed using the MAGPIX (Merck, Darmstadt, Germany) and the xPONENT software (Merck). All values were normalized with total protein concentration measured by using BCA protein assay kit (Thermo Fisher Scientific).

Statistical Analysis

All the results are expressed as the mean ± SEM as indicated. The Student's *t*-test was used for statistical comparison between the groups, and 1-way ANOVA with Tukey-Kramer was used for multiple comparisons. Differences between the means were considered statistically significant when the probability values were less than 0.05.

RESULTS

Suppression of VAP-1/SSAO Activity by Specific Inhibitor RTU-1096 in Plasma and Chorioretinal Tissues

To validate the pharmacologic effects of RTU-1096, a novel inhibitor for VAP-1/SSAO, we measured SSAO activity in plasma and chorioretinal tissue samples in mice. The SSAO activity was not elevated in plasma samples from the laser group (5.8 ± 0.1 pmol/μg protein/min, $n = 10$) compared with in those from the control group (5.3 ± 0.3 pmol/μg protein/min, $n = 10$, $P = 0.09$, Fig. 2A). The plasma SSAO activity was significantly lower in the plasma of animal groups treated with RTU-1096 (1.9 ± 0.3 pmol/μg protein/min, $n = 10$, $P < 0.01$, Fig. 2A) than that from the laser group.

In chorioretinal tissues, the SSAO activity showed a significant increase in the laser group (1.30 ± 0.08 pmol/mg protein/min, $n = 18$) compared with that in the control group (1.05 ± 0.05 pmol/mg protein/min, $n = 18$, $P < 0.05$, Fig. 2B). The RTU-1096–treated group showed a significant reduction in SSAO activity (0.71 ± 0.04 pmol/mg protein/min, $n = 19$, $P < 0.01$, Fig. 2B) in the chorioretinal tissues compared with in the laser group.

Impact of VAP-1/SSAO Blockade on ONL Thickening Caused by Laser Photocoagulation

To determine whether peripheral retinal laser photocoagulation causes morphologic alteration of retinal structures in the region without photocoagulation with time, total retinal thickness and individual retinal layer thickness were measured using the high-resolution OCT system Spectralis (Fig. 3A). At the baseline, there was no difference in total retinal thickness between the groups (Fig. 3B). However, the groups subjected to laser photocoagulation, that is, laser group ($n = 20$) and RTU-1096 group ($n = 18$), showed a significant decrease in total retinal thickness at 3 and 7 days after laser photocoagulation in comparison with the control group ($n = 19$, $P < 0.01$ each, Fig. 3B). There was no difference in total retinal thickness between laser group and RTU-1096 group at 3 and 7 days after laser photocoagulation (Fig. 3B).

Next, the thickness of individual sublayers was evaluated. One day after laser photocoagulation, the ONL thickness was increased in the laser group compared with in the control

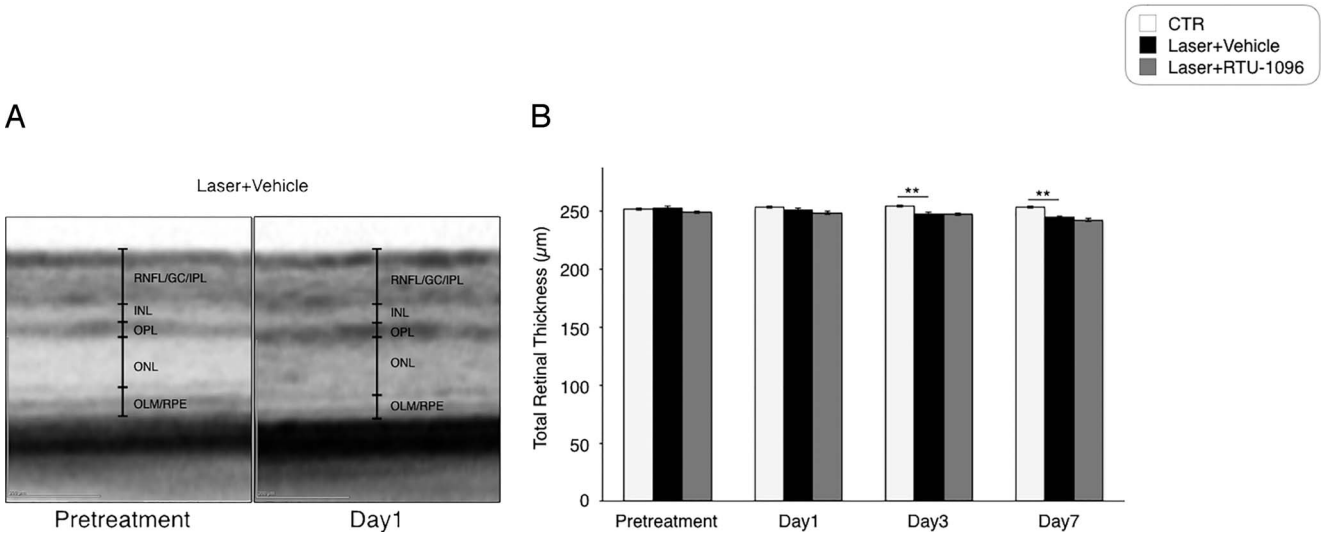

Figure 3. Optical coherence tomography image analysis of total retinal thickness. (**A**) Representative OCT images of mouse retina taken before laser photocoagulation and 1 day after laser photocoagulation. Outer nuclear layer thickness 1 day after laser photocoagulation is increased compared with that of baseline. (**B**) Chronologic observation of total retinal thickness before and at 1, 3, and 7 days after laser photocoagulation. Values are mean ± SEM ($n = 18$–20). *$P < 0.05$, **$P < 0.01$.

group ($n = 19$, $P < 0.01$), and RTU-1096 administration abrogated the thickening in ONL ($n = 18$, $P < 0.01$, Fig. 4A). However, the laser photocoagulation groups, including the laser group and the RTU-1096 group, showed significant decreases in ONL thickness in comparison with the control group 7 days after laser photocoagulation (Fig. 4A). In contrast, the OPL thickness in the laser groups was lower than that in the groups treated with RTU-1096 at 1 day after laser photocoagulation ($n = 20$, $P < 0.05$), and the difference between groups was diminished (Fig. 4B). One day after laser photocoagulation, the thickness of the OLM/RPE complex decreased in the groups having undergone laser photocoagulation regardless of RTU-1096 treatment ($P < 0.01$); however, the thickness recovered by day 7 (Fig. 4C). Throughout the experiment, the thickness of the inner retinal sublayers including the RNFL/GCL/IPL complex and INL were not statistically different between the groups at any time points (Figs. 4D, 4E).

Impact of VAP-1/SSAO Blockade on Leukocyte Accumulation in Eyes After Laser Photocoagulation

Chronologic observation of the retinal sublayer thickness using OCT indicated that peripheral retinal laser photocoagulation elicited the acute biological response of ONL thickening, which was inhibited by blocking VAP-1/SSAO, 1 day after laser photocoagulation. To investigate whether VAP-1 blockade suppresses intraocular inflammation caused by laser photocoagulation, we quantified the cumulative number of transmigrated leukocytes in the vitreous, 1 day after laser photocoagulation.

The number of the inflammatory cells significantly increased in the vitreous in the laser group (50.1 ± 1.3 cells/section, $n = 4$), when compared with that in the control group (0.4 ± 0.4 cells/section, $n = 4$, $P < 0.01$, Figs. 5A, 5B). However, in the RTU-1096–treated group, the leukocyte infiltration was significantly suppressed (31.2 ± 7.7 cells/section, $n = 4$, $P < 0.05$, Figs. 5A, 5B) in comparison to that in the laser group. In parallel with the H&E staining data, whereas the control group showed no or very few hyperreflective foci at vitreoretinal interface in OCT images (0.4 ± 0.2 dots/image, $n = 12$), there was a high number of the hyperreflective foci in the laser group (31.7 ± 2.4 dots/image, $n = 16$, $P < 0.01$, Figs. 5C, 5D). In the RTU-1096 group, the hyperreflective foci were reduced by 29% compared with those in the laser group (22.5 ± 2.3 dots/image, $n = 14$, $P < 0.05$, Figs. 5C, 5D).

Impact of VAP-1/SSAO Blockade on Endothelial Adhesion Molecule ICAM-1 in the Retina After Laser Photocoagulation

To further analyze the mechanism by which VAP-1 blockade attenuates inflammatory cell migration after peripheral laser photocoagulation, we examined *ICAM-1* expression levels in the animal retinal tissues and assessed the effect of the VAP-1/SSAO inhibitor on their expressions. The retinal *ICAM-1* expression level showed an 8.6-fold increase in the laser group ($n = 12$) compared with that in the control group ($n = 12$, $P < 0.01$, Fig. 6A). In the VAP-1 inhibitor–treated animals, *ICAM-1* mRNA expression was downregulated in comparison with the laser group (Fig. 6A). Protein level of retinal ICAM-1 increased in the laser group ($n = 9$, 8.5 pg/mg) compared with control group ($n = 10$, 4.0 pg/mg, $P < 0.01$, Fig. 6B). In the RTU-1096 group, the retinal ICAM-1 protein was reduced in comparison with those in the laser group ($n = 12$, 7.0 pg/mg, $P < 0.01$, Fig. 6B).

Discussion

In the present study, we demonstrated that peripheral retinal photocoagulation causes (1) transient ONL thickening in the proximal remote region, (2) leukocyte infiltration at the vitreoretinal surface, and (3) upregulation of the leukocyte adhesion molecule ICAM-1 in the retina. Furthermore, as a novel finding, we showed that the VAP-1/SSAO inhibitor RTU-1096 reduced these biological responses caused by laser photocoagulation. The current data indicate that VAP-1/SSAO inhibition may be a potential therapeutic strategy for the prevention of ME secondary to scatter laser photocoagulation in patients with ischemic retinal diseases, such as PDR.

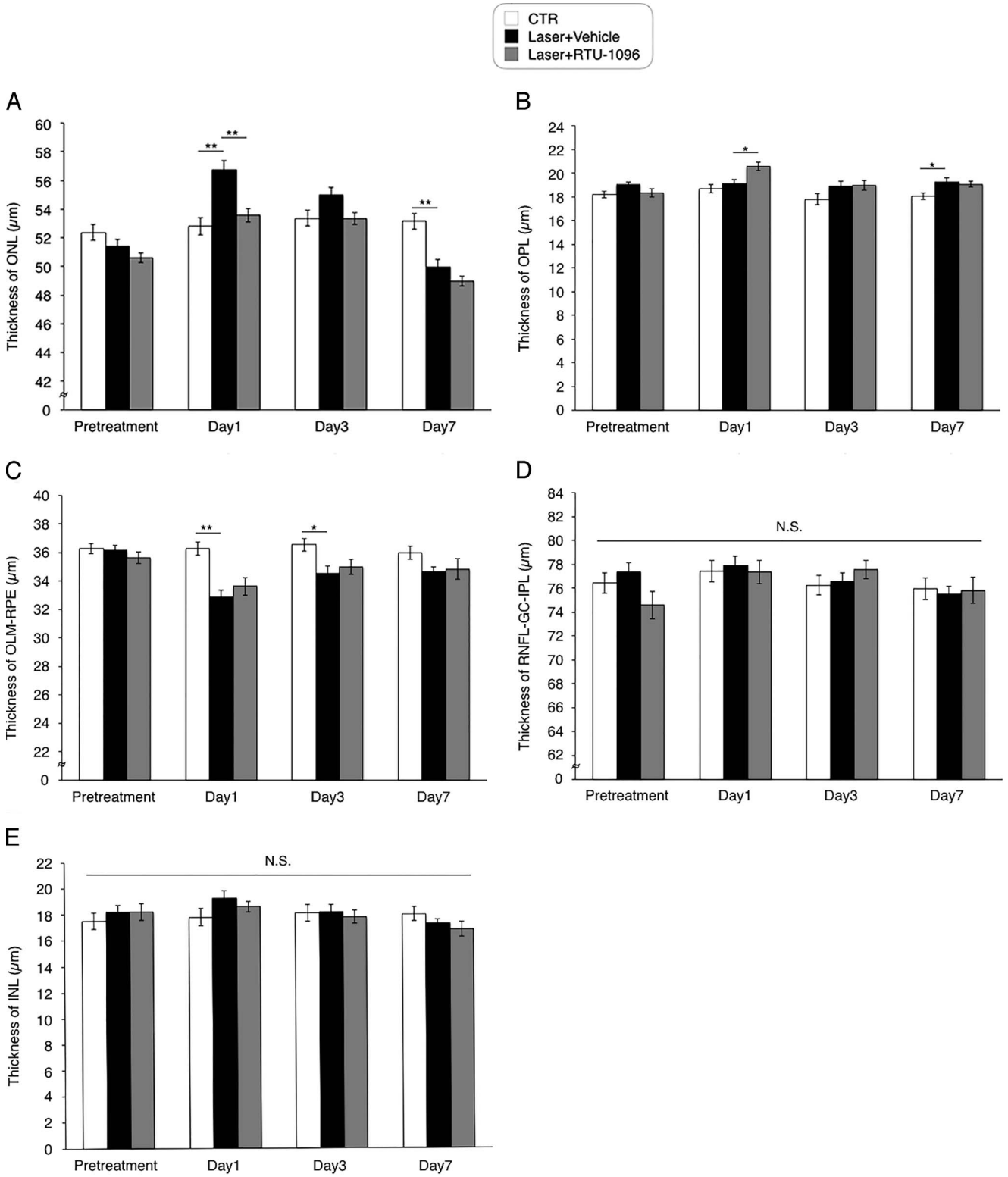

FIGURE 4. Optical coherence tomography image analysis of retinal sublayer thickness. The thickness of individual retinal sublayers was chronologically evaluated before laser photocoagulation and at 1, 3, and 7 days after laser photocoagulation. (**A**) Outer nuclear layer. (**B**) Outer plexiform layer. (**C**) The complex from OLM/RPE. (**D**) The combination of RNFL/GC/IPL. (**E**) Inner nuclear layer. Values are mean ± SEM ($n = 18$–20). $^{*}P < 0.05$, $^{**}P < 0.01$.

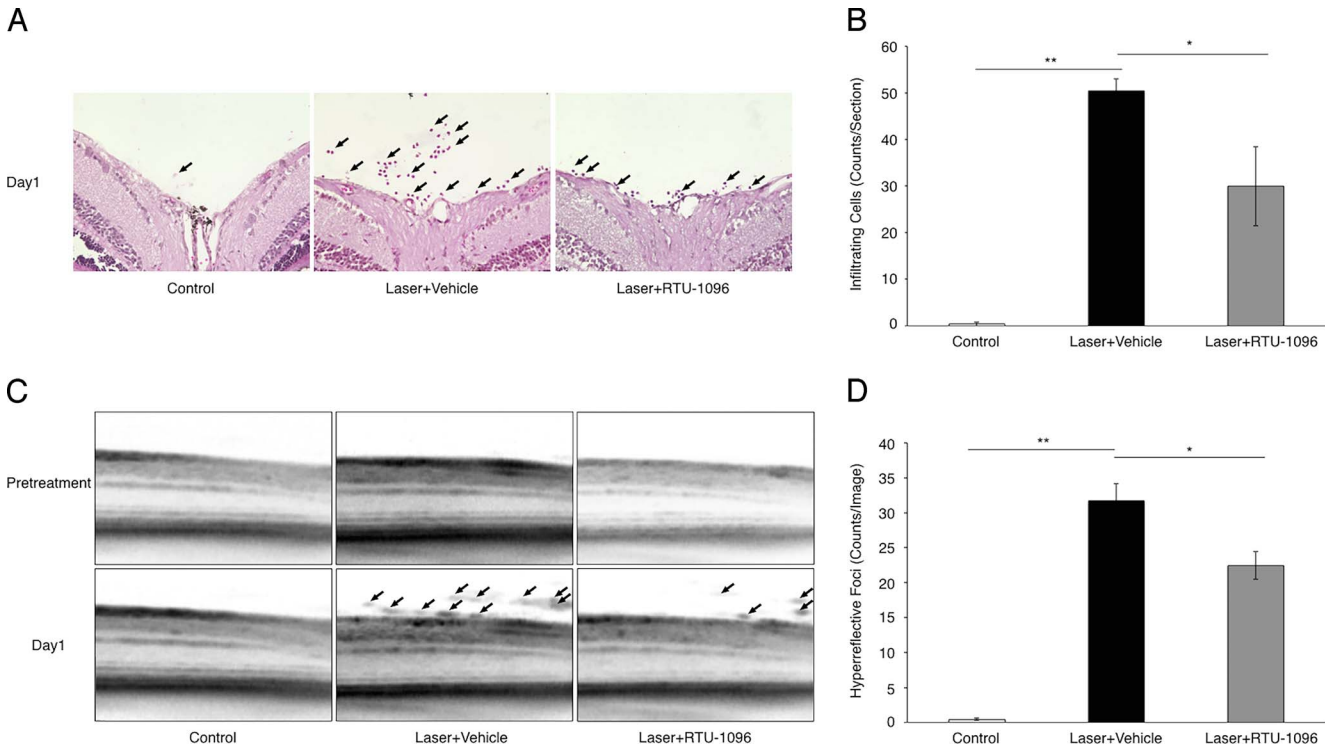

Figure 5. Impact of VAP-1/SSAO inhibition on intraocular leukocyte accumulation caused by laser photocoagulation. (**A**) Representative micrographs of H&E staining obtained from control and laser-treated animals with or without VAP-1 inhibitor treatment. *Arrows* indicate infiltrated leukocytes in the retina. (**B**) The number of infiltrated leukocytes in the vitreous with or without VAP-1 inhibitor treatment. Values are mean ± SEM ($n = 4$). $^{*}P < 0.05$, $^{**}P < 0.01$. (**C**) Representative OCT images obtained from control and laser-treated animals with or without VAP-1 inhibitor treatment. *Arrows* indicate hyperreflective foci observed at the vitreoretinal surface. (**D**) The number of hyperreflective foci at the vitreoretinal surface with or without VAP-1 inhibitor treatment. Values are mean ± SEM ($n = 12$–16). $^{*}P < 0.05$, $^{**}P < 0.01$.

To date, histologic analysis has been used for chronologic observation of the posterior segment of the eye in animal experiments; however, this procedure requires animal killing and an immense amount of time. The OCT instrument enables, in addition to substantial time saving, close analysis of the sequential alteration of intraocular findings with time in in vivo experiments. In previous studies, total retinal thickness in C57BL/6 mice ranged from approximately 250 to 300 μm,[26–28] and total retinal thickness of untreated mice measured in this study was in this range, indicating that the OCT system Spectralis is useful to chronologically evaluate the retinal thickness in mice.

Using the high-resolution OCT system, we found the transient increase of ONL thickness and the decrease of OLM/RPE complex thickness at the earliest time point after laser photocoagulation. Whereas scatter laser photocoagulation was reported to progressively reduce the thickness of the inner retina in patients with DME,[29–31] transient ONL thickening at 1 day after laser photocoagulation was also documented in patients with DME.[32] Furthermore, Mitsch et

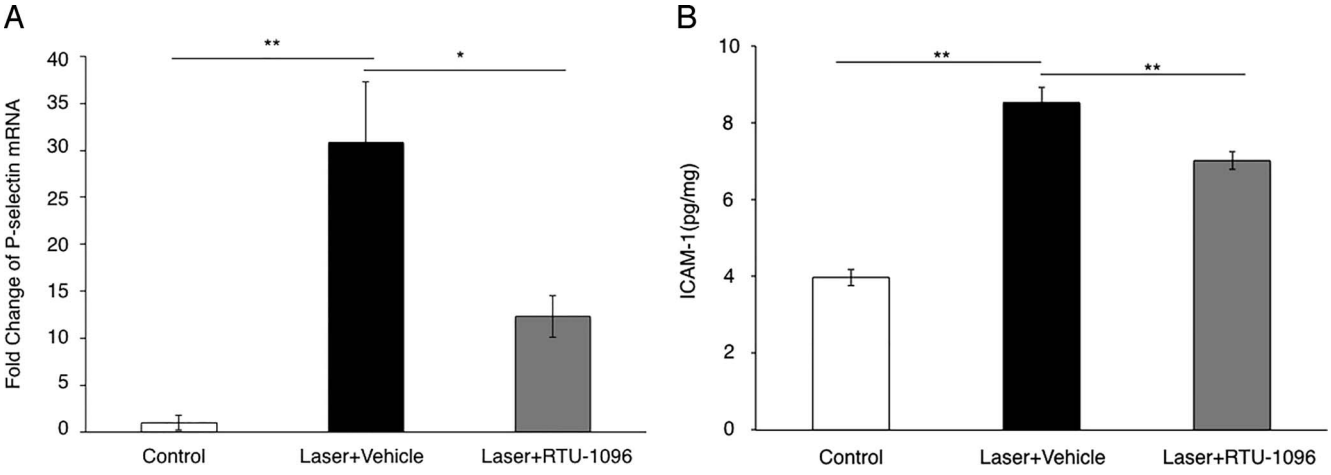

Figure 6. Role of VAP-1 inhibition on retinal ICAM-1 after laser photocoagulation. (**A**) Quantitative real-time PCR analysis for the endothelial adhesion molecule *ICAM-1* in the retinas of laser-treated animals with or without VAP-1 inhibitor treatment. Values are mean ± SEM ($n = 10$–12). $^{*}P < 0.05$, $^{**}P < 0.01$. (**B**) Magnetic luminex assay for retinal ICAM-1 protein. Values are mean ± SEM ($n = 9$–12). $^{**}P < 0.01$.

al.[33] reported that scatter laser photocoagulation leads to a decrease of thickness in the photoreceptor and RPE layers in cases with PDR in addition to the ONL swelling. Similarly, in the current study, the acute ONL swelling and the OLM/RPE complex thinning were seen in the outer retinal layers of mice 1 day after laser photocoagulation. In addition, the animals treated with VAP-1/SSAO inhibitor showed increase of both OPL and OLM-RPE compared with the nontreated animals. Presumably, the suppressive effect of the inhibitor on laser-induced ONL thickening reduced the changes in the OPL and OLM-RPE layers adjacent to ONL. The current animal study and the clinical findings indicate that scatter laser photocoagulation causes acute morphologic alterations in retinal layers.

It was recently demonstrated that inflammatory mediators such as cytokines and leukocyte adhesion molecules were upregulated in the rabbit retina 1 day after laser photocoagulation.[23] Hence, the transient changes of outer retinal layers might be the consequence of an inflammatory response that spreads from the laser-treated area. In support of this hypothesis, ICAM-1 was significantly upregulated in the retina of animals having undergone laser photocoagulation at day 1 in the current study. Previously, we reported the increased retinal expression level of ICAM-1 in an acute intraocular inflammation model.[20] The current and previous data indicate that ICAM-1 is a molecule inducible by inflammation. Additionally, histologic analysis also revealed that laser photocoagulation increased the number of infiltrated leukocytes in the vitreous cavity and the retinal tissues. Therefore, it is presumable that laser photocoagulation causes retinal ICAM-1 upregulation, leading to the increase in leukocyte recruitment.

The VAP-1/SSAO inhibitor RTU-1096 reduced intraocular leukocyte recruitment into the vitreous after laser photocoagulation. Because VAP-1 is a leukocyte adhesion molecule that regulates transmigration step of leukocytes, it is likely that the reduction of postlaser leukocyte infiltration into the vitreous by VAP-1 inhibitor RTU-1096 is a consequence of direct effect on VAP-1. However, it is noted that the VAP-1/SSAO inhibitor RTU-1096 also reduced the expression of ICAM-1 caused by peripheral laser photocoagulation. Vascular adhesion protein-1/SSAO is an enzyme that generates the corresponding aldehyde, hydrogen peroxide, and ammonium. Previously, it was reported that hydrogen peroxide augments ICAM-1 expression in endothelial cells.[34,35] Therefore, the reduced ICAM-1 expression with VAP-1 blockade may be partially due to reduced hydrogen peroxide.

In addition, the inhibitor RTU-1096 ameliorated transient ONL thickening, possibly due to inflammatory responses caused by laser photocoagulation in the photoreceptors. The morphologic change in ONL is associated with visual prognosis in patients with DME.[36,37] Similarly, ONL integrity is crucial for visual prognosis in other types of retinal diseases, such as central serous chorioretinopathy[38] and AMD.[39] Therefore, the current data may indicate that blockage of VAP-1/SSAO is beneficial to avoid visual function loss after laser photocoagulation. Further functional analysis is required to investigate the effect of the VAP-1/SSAO inhibitor on the visual function of mice after peripheral laser photocoagulation.

In summary, peripheral retinal photocoagulation causes transient morphologic changes in the outer retina and leukocyte infiltration into ocular tissues. Vascular adhesion protein-1 blockade with a novel and specific inhibitor potently suppresses the inflammatory response and transient ONL thickening after scatter laser photocoagulation. Previously, it was reported that oral administration of a VAP-1 inhibitor prevented retinal vascular permeability in a streptozotocin-induced diabetic model.[40] These findings suggest VAP-1 inhibition as a novel and potent therapeutic strategy in ME secondary to laser photocoagulation in patients with DR.

Acknowledgments

The authors thank Ikuyo Hirose, Shiho Yoshida, and Erdal Tan Ishizuka for their skillful technical assistance.

Supported by a Grant-in-Aid for Scientific Research (C) 17K11444, 15K10855, 26462657 (KN); 17K11442 (MM); from the Japan Society for the Promotion of Science (Tokyo, Japan), and funded by Sucampo Pharma, LLC (Tokyo, Japan).

Disclosure: **T. Matsuda**, None; **K. Noda**, Sucampo Pharma, LLC (F); **M. Murata**, None; **A. Kawasaki**, Sucampo Pharma, LLC (E); **A. Kanda**, None; **Y. Mashima**, None; **S. Ishida**, None

References

1. Cheung N, Mitchell P, Wong TY. Diabetic retinopathy. *Lancet*. 2010;376:124–136.
2. Lee R, Wong TY, Sabanayagam C. Epidemiology of diabetic retinopathy, diabetic macular edema and related vision loss. *Eye Vis (Lond)*. 2015;2:17.
3. Funatsu H, Yamashita H, Ikeda T, Mimura T, Eguchi S, Hori S. Vitreous levels of interleukin-6 and vascular endothelial growth factor are related to diabetic macular edema. *Ophthalmology*. 2003;110:1690–1696.
4. Funatsu H, Yamashita H, Noma H, Mimura T, Yamashita T, Hori S. Increased levels of vascular endothelial growth factor and interleukin-6 in the aqueous humor of diabetics with macular edema. *Am J Ophthalmol*. 2002;133:70–77.
5. Adamis AP, Miller JW, Bernal MT, et al. Increased vascular endothelial growth factor levels in the vitreous of eyes with proliferative diabetic retinopathy. *Am J Ophthalmol*. 1994; 118:445–450.
6. Lebherz C, Maguire AM, Auricchio A, et al. Nonhuman primate models for diabetic ocular neovascularization using AAV2-mediated overexpression of vascular endothelial growth factor. *Diabetes*. 2005;54:1141–1149.
7. Heier JS, Korobelnik JF, Brown DM, et al. Intravitreal aflibercept for diabetic macular edema: 148-week results from the VISTA and VIVID studies. *Ophthalmology*. 2016;123: 2376–2385.
8. Ip MS, Domalpally A, Sun JK, Ehrlich JS. Long-term effects of therapy with ranibizumab on diabetic retinopathy severity and baseline risk factors for worsening retinopathy. *Ophthalmology*. 2015;122:367–374.
9. Simunovic MP, Maberley DA. Anti-vascular endothelial growth factor therapy for proliferative diabetic retinopathy: a systematic review and meta-analysis. *Retina*. 2015;35:1931–1942.
10. The Diabetic Retinopathy Study Research Group. Preliminary report on effects of photocoagulation therapy. *Am J Ophthalmol*. 1976;81:383–396.
11. The Diabetic Retinopathy Study Research Group. Four risk factors for severe visual loss in diabetic retinopathy. The third report from the Diabetic Retinopathy Study. *Arch Ophthalmol*. 1979;97:654–655.
12. British Multicentre Study Group. Photocoagulation for proliferative diabetic retinopathy: a randomised controlled clinical trial using the xenon-arc. *Diabetologia*. 1984;26:109–115.
13. Paulus YM, Jain A, Gariano RF, et al. Healing of retinal photocoagulation lesions. *Invest Ophthalmol Vis Sci*. 2008; 49:5540–5545.
14. McDonald HR, Schatz H. Macular edema following panretinal photocoagulation. *Retina*. 1985;5:5–10.
15. Shimura M, Yasuda K, Nakazawa T, Kano T, Ohta S, Tamai M. Quantifying alterations of macular thickness before and after panretinal photocoagulation in patients with severe diabetic

retinopathy and good vision. *Ophthalmology*. 2003;110: 2386–2394.

16. Googe J, Brucker AJ, Bressler NM, et al.; for the Diabetic Retinopathy Clinical Research Network. Randomized trial evaluating short-term effects of intravitreal ranibizumab or triamcinolone acetonide on macular edema after focal/grid laser for diabetic macular edema in eyes also receiving panretinal photocoagulation. *Retina*. 2011;31:1009–1027.
17. Sheyman AT, Cohen BZ, Friedman AH, Ackert JM. An outbreak of fungal endophthalmitis after intravitreal injection of compounded combined bevacizumab and triamcinolone. *JAMA Ophthalmol*. 2013;131:864–869.
18. Salmi M, Jalkanen S. A 90-kilodalton endothelial cell molecule mediating lymphocyte binding in humans. *Science*. 1992;257: 1407–1409.
19. Salmi M, Jalkanen S. VAP-1: an adhesin and an enzyme. *Trends Immunol*. 2001;22:211–216.
20. Noda K, Miyahara S, Nakazawa T, et al. Inhibition of vascular adhesion protein-1 suppresses endotoxin-induced uveitis. *FASEB J*. 2008;22:1094–1103.
21. Noda K, Nakao S, Zandi S, Engelstadter V, Mashima Y, Hafezi-Moghadam A. Vascular adhesion protein-1 regulates leukocyte transmigration rate in the retina during diabetes. *Exp Eye Res*. 2009;89:774–781.
22. Salmi M, Jalkanen S. Cell-surface enzymes in control of leukocyte trafficking. *Nat Rev Immunol*. 2005;5:760–771.
23. Arimura S, Takamura Y, Miyake S, et al. The effect of triamcinolone acetonide or bevacizumab on the levels of proinflammatory cytokines after retinal laser photocoagulation in pigmented rabbits. *Exp Eye Res*. 2016;149:1–7.
24. Chidlow G, Shibeeb O, Plunkett M, Casson RJ, Wood JP. Glial cell and inflammatory responses to retinal laser treatment: comparison of a conventional photocoagulator and a novel, 3-nanosecond pulse laser. *Invest Ophthalmol Vis Sci*. 2013;54: 2319–2332.
25. Ehrlich R, Harris A, Ciulla TA, Kheradiya N, Winston DM, Wirostko B. Diabetic macular oedema: physical, physiological and molecular factors contribute to this pathological process. *Acta Ophthalmol*. 2010;88:279–291.
26. Dysli C, Enzmann V, Sznitman R, Zinkernagel MS. Quantitative analysis of mouse retinal layers using automated segmentation of spectral domain optical coherence tomography images. *Trans Vis Sci Tech*. 2015;4(4):9.
27. Gabriele ML, Ishikawa H, Schuman JS, et al. Reproducibility of spectral-domain optical coherence tomography total retinal thickness measurements in mice. *Invest Ophthalmol Vis Sci*. 2010;51:6519–6523.
28. Shariati MA, Park JH, Liao YJ. Optical coherence tomography study of retinal changes in normal aging and after ischemia. *Invest Ophthalmol Vis Sci*. 2015;56:2790–2797.
29. Kim JJ, Im JC, Shin JP, Kim IT, Park DH. One-year follow-up of macular ganglion cell layer and peripapillary retinal nerve fibre layer thickness changes after panretinal photocoagulation. *Br J Ophthalmol*. 2014;98:213–217.
30. Lim MC, Tanimoto SA, Furlani BA, et al. Effect of diabetic retinopathy and panretinal photocoagulation on retinal nerve fiber layer and optic nerve appearance. *Arch Ophthalmol*. 2009;127:857–862.
31. Muqit MM, Wakely L, Stanga PE, Henson DB, Ghanchi FD. Effects of conventional argon panretinal laser photocoagulation on retinal nerve fibre layer and driving visual fields in diabetic retinopathy. *Eye (Lond)*. 2010;24:1136–1142.
32. Deak GG, Bolz M, Kriechbaum K, et al. Effect of retinal photocoagulation on intraretinal lipid exudates in diabetic macular edema documented by optical coherence tomography. *Ophthalmology*. 2010;117:773–779.
33. Mitsch C, Pemp B, Kriechbaum K, Bolz M, Scholda C, Schmidt-Erfurth U. Retinal morphometry changes measured with spectral domain-optical coherence tomography after pan-retinal photocoagulation in patients with proliferative diabetic retinopathy. *Retina*. 2016;36:1162–1169.
34. Lakshminarayanan V, Beno DW, Costa RH, Roebuck KA. Differential regulation of interleukin-8 and intercellular adhesion molecule-1 by H2O2 and tumor necrosis factor-alpha in endothelial and epithelial cells. *J Biol Chem*. 1997; 272:32910–32918.
35. Lo SK, Janakidevi K, Lai L, Malik AB. Hydrogen peroxide-induced increase in endothelial adhesiveness is dependent on ICAM-1 activation. *Am J Physiol*. 1993;264:L406–L412.
36. Deak GG, Bolz M, Ritter M, et al. A systematic correlation between morphology and functional alterations in diabetic macular edema. *Invest Ophthalmol Vis Sci*. 2010;51:6710–6714.
37. Reznicek L, Cserhati S, Seidensticker F, et al. Functional and morphological changes in diabetic macular edema over the course of anti-vascular endothelial growth factor treatment. *Acta Ophthalmol*. 2013;91:e529–e536.
38. Ohkuma Y, Hayashi T, Sakai T, Watanabe A, Tsuneoka H. One-year results of reduced fluence photodynamic therapy for central serous chorioretinopathy: the outer nuclear layer thickness is associated with visual prognosis. *Graefes Arch Clin Exp Ophthalmol*. 2013;251:1909–1917.
39. Pappuru RR, Ouyang Y, Nittala MG, et al. Relationship between outer retinal thickness substructures and visual acuity in eyes with dry age-related macular degeneration. *Invest Ophthalmol Vis Sci*. 2011;52:6743–6748.
40. Inoue T, Morita M, Tojo T, et al. Synthesis and SAR study of new thiazole derivatives as vascular adhesion protein-1 (VAP-1) inhibitors for the treatment of diabetic macular edema: part 2. *Bioorg Med Chem*. 2013;21:2478–2494.

Investigative Ophthalmology & Visual Science